AD-A080 246 DAVID W TAYLOR NAVAL SHIP RESEARCH AND DEVELOPMENT CE--ETC F/G 11/6
FATIGUE CRACK GROWTH IN WELDBONDED ALUMINUM ALLOY STIFFENED PAN--ETC(U)
DEC 79 H P CHU, J A HAUSER, J P SIKORA
UNCLASSIFIED DTNSRDC-79/102 NL

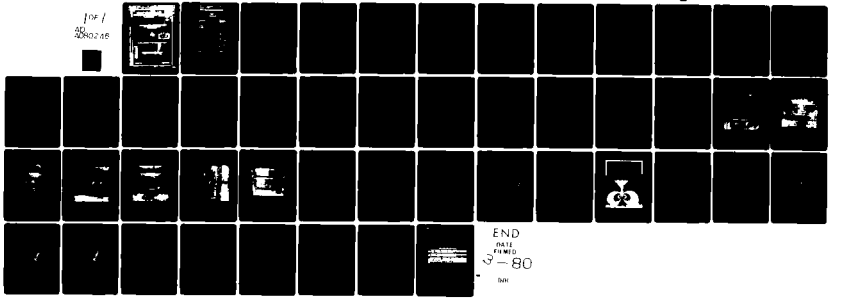

END
DATE FILMED
2-80
DDC

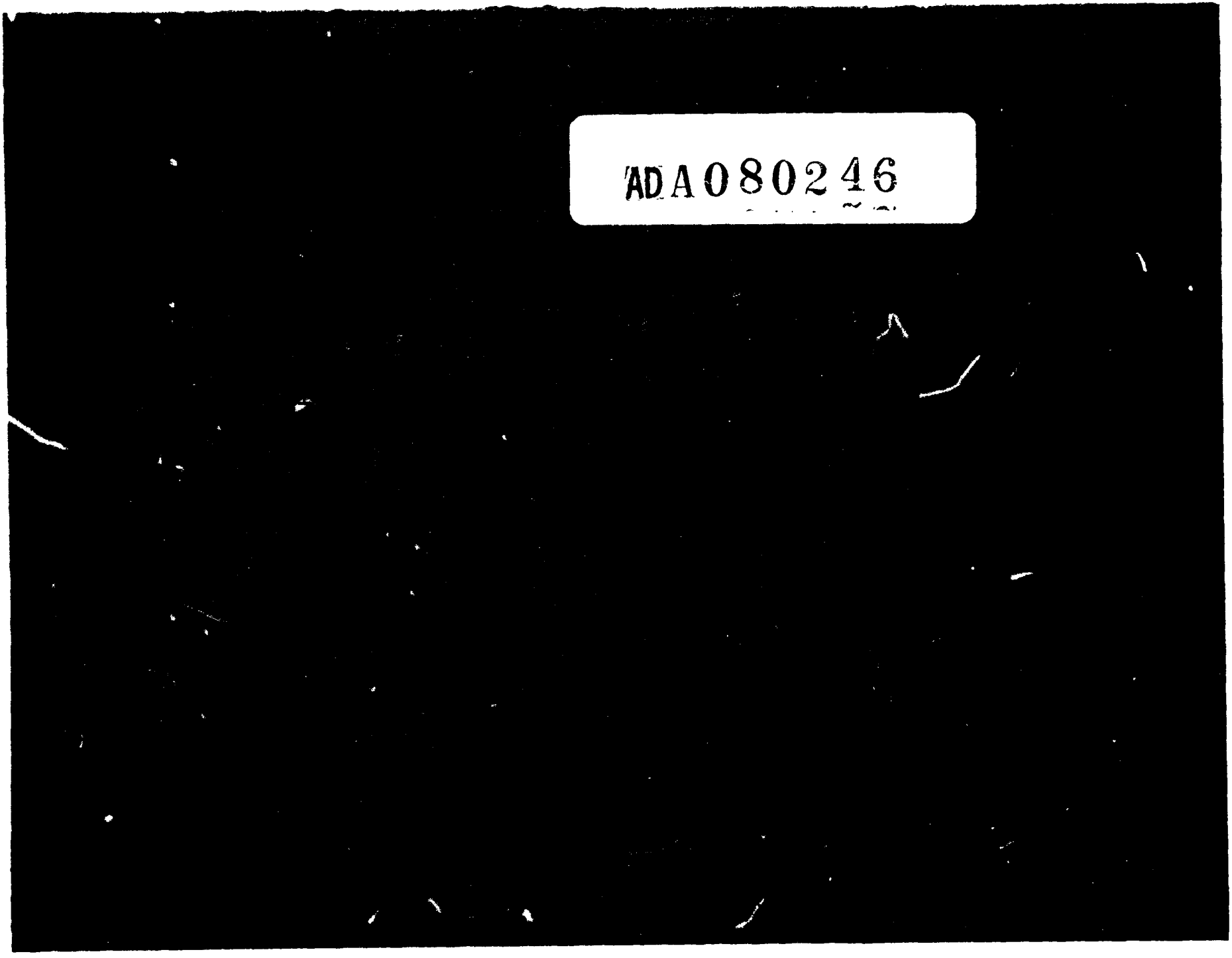

UNCLASSIFIED

SECURITY CLASSIFICATION OF THIS PAGE (When Data Entered)

REPORT DOCUMENTATION PAGE

READ INSTRUCTIONS BEFORE COMPLETING FORM

1. REPORT NUMBER	2. GOVT ACCESSION NO.	3. RECIPIENT'S CATALOG NUMBER
DTNSRDC-79/102		

4. TITLE (and Subtitle)

FATIGUE CRACK GROWTH IN WELDBONDED ALUMINUM ALLOY STIFFENED PANELS UNDER PRESSURE LOADING.

5. TYPE OF REPORT & PERIOD COVERED
Research & Development

6. PERFORMING ORG. REPORT NUMBER

7. AUTHOR(s)
H. P. Chu, J. A. Hauser, and J. P. Sikora

8. CONTRACT OR GRANT NUMBER(s)

9. PERFORMING ORGANIZATION NAME AND ADDRESS
David W. Taylor Naval Ship R&D Center
Bethesda, MD 20084

10. PROGRAM ELEMENT, PROJECT, TASK AREA & WORK UNIT NUMBERS
(See reverse side)

11. CONTROLLING OFFICE NAME AND ADDRESS
Naval Sea Systems Command (SEA 05R & 32R)
Washington, DC 20362

12. REPORT DATE
December 1979

13. NUMBER OF PAGES
46

14. MONITORING AGENCY NAME & ADDRESS (if different from Controlling Office)

15. SECURITY CLASS. (of this report)
UNCLASSIFIED

15a. DECLASSIFICATION/DOWNGRADING SCHEDULE

16. DISTRIBUTION STATEMENT (of this Report)

APPROVED FOR PUBLIC RELEASE; DISTRIBUTION UNLIMITED

17. DISTRIBUTION STATEMENT (of the abstract entered in Block 20, if different from Report)

18. SUPPLEMENTARY NOTES

19. KEY WORDS (Continue on reverse side if necessary and identify by block number)

Fatigue
Fracture Mechanics
Crack Growth
Aluminum Alloy
Stiffened Panels
Weldbonding

20. ABSTRACT (Continue on reverse side if necessary and identify by block number)

An experimental study was conducted to characterize the fatigue crack growth behavior of stiffened panels under uniform lateral pressure loading. The panels were made of standard 5456 aluminum alloy and fabricated by weldbonding. Fatigue failure of the panels consisted of cracking of the stiffeners followed by cracking of the skin. Crack growth rate data showed a maximum value in the stiffeners and a constant value in the skin before

(Continued on reverse side)

DD FORM 1 JAN 73 1473 EDITION OF 1 NOV 65 IS OBSOLETE
S/N 0102-LF-014-6601

UNCLASSIFIED

SECURITY CLASSIFICATION OF THIS PAGE (When Data Entered)

(Block 10)

Task Areas SF 43 422 593 & SF 54 59052
Work Units 2814-163 & 1730-593

(Block 20 continued)

failure. A weldbonded stiffened panel could endure more fatigue cycles than a gas metal arc welded panel under similar pressure loading. The panel data were correlated with base line materials data and represented by either of two simple equations in terms of fatigue crack growth rate versus stress intensity factor range. The stress intensity analysis for the panels was made by an approximation method considering the combined effects of tension and bending stresses. Accuracy of this method was verified by photoelastic measurements.

TABLE OF CONTENTS

LIST OF FIGURES

LIST OF TABLES

NOMENCLATURE

a	Crack length
c,m,n	Constants (used in Equations (6) and (7))
F_1,F_2,F_3	Correction factors (used in Equations (2), (3), and (4))
h	Plate thickness
K	Stress intensity factor
K_c	Critical value of stress intensity factor (fracture toughness)
$\overline{K}_j$	Component of K due to Q_j
M	Bending moment
Q_j	Rivet forces
R	Stress ratio
r,ϕ,θ	Polar coordinates
S_b	Bending stress
S_t	Tensile stress
ΔK	Stress intensity factor range
ΔK_{th}	Fatigue threshold of ΔK
σ_o	Far-field stress
τ_{max}	Maximum shear stress

LIST OF ABBREVIATIONS

ASTM	American Society of Testing and Materials
CT	Compact tension
GMA	Gas metal arc
Hz	Hertz (cycle per second)
ksi	Thousand pounds per square inch
m	Meter
mm	Millimeter
MPa	Megapascal
psig	Pound per square inch gage

ABSTRACT

An experimental study was conducted to characterize the fatigue crack growth behavior of stiffened panels under uniform lateral pressure loading. The panels were made of standard 5456 aluminum alloy and fabricated by weldbonding. Fatigue failure of the panels consisted of cracking of the stiffeners followed by cracking of the skin. Crack growth rate data showed a maximum value in the stiffeners and a constant value in the skin before failure. A weldbonded stiffened panel could endure more fatigue cycles than a gas metal arc welded panel under similar pressure loading. The panel data were correlated with base line materials data and represented by either of two simple equations in terms of fatigue crack growth rate versus stress intensity factor range. The stress intensity analysis for the panels was made by an approximation method considering the combined effects of tension and bending stresses. Accuracy of this method was verified by photoelastic measurements.

ADMINISTRATIVE INFORMATION

This is the summary report on work accomplished under funding by the Naval Sea Systems Command (SEA 32R and 05R) under Task Area SF 43 422 593 (Work Unit 1730-593) and Task Area SF 54 59052 (Work Unit 2814-163). Program managers were Mr. C. H. Pohler (NAVSEA, SEA 32R) and Dr. H. H. Vanderveldt (NAVSEA, SEA 05R).

INTRODUCTION

Stiffened panels are extensively used as structural elements in the construction of high performance ships. Previous work on stiffened panels was limited to uniaxial tensile loading. For example, Poe and Vlieger[1,2*] studied their fatigue crack growth and residual strength characteristics under simple tension. This work was different from others in that the panels were tested in bending. The purpose was to investigate fatigue crack growth in aluminum alloy stiffened panels under uniform lateral

*A complete listing of references is given on page 37.

loading similar to the water pressure experienced by ship structures, such that the data would be useful for controlling fatigue and fracture in modern ships as discussed by Sorkin, Wolfe, Vanderveldt, and others.[3,4] The technical approach was based on the fracture mechanics concept that fatigue crack propagation in structural elements can be predicted from base line materials data in terms of the linear elastic stress intensity factor range ΔK versus crack growth rate da/dN, as shown by Paris and Wei.[5,6]

EXPERIMENTAL PROCEDURE

MATERIALS

The stiffened panels tested were made of a standard Al-Mg alloy. The skin material was 5456-H343 sheet, and the stiffeners were 5456-H111 extrusions. All the materials were 0.125 in. (3.2 mm)* thick and tested in the as-received condition. Chemical composition and mechanical properties are listed in Table 1.

TABLE 1 - CHEMICAL COMPOSITION AND MECHANICAL PROPERTIES OF 5456 ALUMINUM ALLOY

Temper	Chemical Composition, weight %								Mechanical Properties			
									0.2% Yield Strength		Tensile Strength	
	Mg	Mn	Fe	Cr	Ti	Zn	Si	Al	ksi	MPa	ksi	MPa
H343	6.0	0.91	0.33	0.13	0.06	0.05	0.01	Bal	40.3	278	56.4	389
H111	5.4	1.0	0.32	0.13	0.07	0.02	0.01	Bal	26.0	179	42.1	290

*Definitions of abbreviations used are given on page vii.

STIFFENED PANEL FABRICATION AND TESTING

Three aluminum alloy stiffened panels were fabricated by weldbonding. Figure 1 shows the dimensions of the panels, which were designed to have the necessary details of a structural element in a simple configuration.[7] The weldbonding process, which was performed by Sciaky Bros., Inc., Chicago, used adhesive EC2214 and spot welded the flanges of the inverted tee stiffeners to the base plate. Two of the weldbonded panels had 0.05-in. (1.27-mm)-deep notches cut by a jeweler's saw at the midpoint of the free edge of the stiffeners. The third panel was not prenotched so that fatigue cracks could follow their natural courses of initiation and propagation.

A special fatigue machine was used to provide lateral loading by compressed air from zero to preselected gage pressures (R = 0) at a speed of 0.2 Hz with the panel supported and constrained along the two edges perpendicular to the stiffeners (Figure 1b). The operation and loading method of a similar machine have been described previously by Cordiano.[8] Before testing, rectangular rosette strain gages were placed on the top and bottom surfaces in the center of all the panels to measure strains from which the applied stresses were calculated. Crack length measurements were taken with a 10X microscope.

The pressure and the initial stresses for the panels are listed in Table 2. Included in this table are the data of two additional panels of the same materials and configuration, which were made by conventional GMA welding of two bar stiffeners using 5356 aluminum wire (Figure 2). The GMA panels were tested previously[9] in the same way as the weldbonded panels, and the results are included here for comparison.

PHOTOELASTIC STRESS INTENSITY MEASUREMENTS

Another GMA welded panel similar to that shown in Figure 2 was used for photoelastic measurements of stress intensity factors. A photoelastic coating was cemented to the top center portion of the panel and also to the sides of the stiffeners. The panel was mounted on a load frame, with the two edges perpendicular to the stiffeners supported and constrained

TABLE 2 - SUMMARY OF STIFFENED PANEL CYCLIC PRESSURE LOADS AND INITIAL STRESSES

Panel No.	Panel Type	Cyclic Pressure		Initial Stress			
				Tension		Compression	
		psig	MPa	ksi	MPa	ksi	MPa
I	Weld Bond	0-20	0-0.138	20.1	138.6	-7.0	-48.3
II*	Weld Bond	0-20	0-0.138	20.0	137.9	-7.0	-48.3
III*	Weld Bond	0-8	0-0.055	11.4	78.6	-5.6	-38.6
IV	GMA Weld	0-20	0-0.138	26.6	183.4	-8.2	-56.5
V	GMA Weld	0-8	0-0.055	18.1	124.8	-12.3	-85.1

*Panel with prenotched stiffeners.

by bolts. To simulate crack growth in fatigue testing, notches were cut in small increments with a hacksaw blade and then sharpened by a knife edge. The cuts started from the free edges of both stiffeners at the midpoint, extended to the base, and then continued through the skin material along the transverse center line of the panel. The load was applied normal to the central area of the bottom surface of the panel. Photoelastic and strain gage readings as well as dial-gage deflection measurements at the center of the panel were taken at each increment of the notching process.

RESULTS AND DISCUSSION

FATIGUE CRACKING IN STIFFENED PANELS

The manner in which the stiffened panels failed in the fatigue tests depended on the fabrication process. The three cracked weldbonded panels

are shown in Figures 3-5. Two photographs are provided for each panel, one for the top and the other for the bottom side. The unique feature is that, after the stiffeners had broken through the flanges, new cracks initiated and propagated in the skin material. In all cases, the cracks in the skin ran through two neighboring weld spots and were not aligned with the cracks in the stiffeners. Also, cracks branched from the spot welds in Panel III (Figure 5b). Irwin[10] has pointed out that many instances of crack branching have been observed and that the branching appears to be related to the attainment of a limiting crack speed in dynamic fracturing. In the present case, crack branching occurred at relatively low speed in the fatigue test, since this particular panel was cycled under 0 to 8 psig (0 to 0.055 MPa) which was the lower pressure load used in the experiment with an initial stress of 11.4 ksi (78.6 MPa). In the case of the GMA welded panels, a crack would start, as expected, at the free edge of each stiffener and propagate into the skin material on both sides of the stiffener. The panels gradually failed as the two central cracks grew toward each other. A photograph of a fatigue cracked GMA welded panel is shown in Figure 6, where the central cracks are labeled by letters B and C. Notice that, as with the weldbonded panels, all the cracks initiated and propagated in the general area along the center line of the panels where the stresses were the highest.

An example of crack growth measurements in prenotched stiffeners is presented in Figure 7. The data show a stage of slowdown in crack propagation in the stiffeners as the crack approaches the base plate. The phenomenon can be better seen in terms of fatigue crack growth rate computed by the ASTM recommended method.[11] In Figure 8 the da/dN values increase continually from the beginning and reach a peak when the crack is about halfway through the stiffener. Thereafter, the crack growth rate decreases as the crack approaches the flange of the stiffener. Although this kind of retardation in crack growth can be readily attributed to the presence of the skin material and the flange of the stiffener, no similar data have been found in the technical literature.

Examples of crack growth data in the skin of the panels are given in Figure 9. The initial part of the data points could be faired into straight lines. This is a unique feature which has been observed in all of the five stiffened panels. Thus, the data indicate that the cracks at first grew at practically constant rates. Afterwards, the cracks grew at increased rates as they approached the central region of the panel. Figure 9 also shows that under identical pressure loading the weldbonded panel sustained almost three times as many pressure cycles as the GMA welded panel. This is simply illustrated by the fact that, when a crack grew to 3 in. (76 mm), the GMA welded panel had endured a total of 24,000 cycles, whereas the weldbonded panel had seen about 67,000 cycles. Previous investigations[12,13] have shown that the weldbond process is superior to riveting or other conventional welding in both static and fatigue tests. It should be noted, however, the difference in fatigue life between Panel I (weldbond) and Panel IV (GMA) is mainly in crack initiation because, once cracking starts, the crack growth rate behavior becomes the same in both types of panels in terms of da/dN versus ΔK. Table 2 shows that the measured stress in Panel I was lower than in Panel IV, most likely due to the additional material of the inverted tee flanges necessary for the weldbonding process. The lower stress should account for part of the longer fatigue life of the weldbonded panel.

STRESS INTENSITY FACTOR

Analytical Method

In order to predict fatigue crack growth in the stiffened panels from base line materials data according to fracture mechanics theory, a stress intensity expression for the panels is needed. Since mathematical solutions are not available for the crack problem of the stiffened panels tested under the present loading condition, an approximate analysis has to be made. This is accomplished by considering the panel skin under combined loading of tension (membrane) and bending stresses. The stress intensity contributions from these stresses are added to obtain the total value of ΔK such that

$$\Delta K_{total} = \Delta K_{tension} + \Delta K_{bending} \tag{1}$$

The tension contribution to ΔK is as follows

$$\Delta K_{tension} = F_1 F_2 \left(S_t \sqrt{\pi a} + \sum_j \bar{K}_j Q_j \right) \tag{2}$$

where F_1 and F_2 are correction factors for a pair of collinear cracks[14] and for a crack in a plate of finite width,[15] respectively. Inside the brackets is the formula from Poe for a stiffened panel with broken stringers.[1,16] The term $S_t \sqrt{\pi a}$ is the familiar K expression for a wide plate with a transverse center crack of length 2a subjected to a uniform tensile stress S_t, and $\bar{K}_j Q_j$ is the component of K due to the rivet forces Q_j. For the present work, a continuous weld is modeled by closely spacing the rivets.

According to Sih,[14] the stress intensity factor for a cracked plate under uniform bending is

$$\Delta K_{bending} = F_3 M \sqrt{\pi a} \tag{3}$$

The bending moment is

$$M = \frac{S_b h^2}{6}$$

Therefore

$$\Delta K_{bending} = F_3 \left(\frac{S_b h^2}{6} \right) \sqrt{\pi a} \tag{4}$$

where S_b is bending stress, h is plate thickness, and F_3 is a function of crack length, plate thickness, and Poisson's ratio. The values of S_b and S_t for Equations (2) and (4) are obtained from the measured stresses by assuming a linear stress distribution through the thickness of the panel as illustrated in Figure 10.

It should be noted that a solution for the stiffeners is not formulated here and that the present solution for the panel skin involves simplifications. For example, Sih's formula is only for a smooth plate, and the effect of broken stringers on bending has to be neglected. Also, because mathematical solutions are unavailable, the presence of two cracks in one plate and the finite width of the plate are not considered in the bending analysis. As shown below, the consequences of these simplifications, which are unavoidable at the present time, can be reconciled, and the method of analysis does provide a close correlation between the stiffened panel and the materials data.

Experimental Method

In the photoelastic experiment, the load was scaled to produce deformation in the panel equivalent to that produced in Panel V under 8-psig (0.055-MPa) uniform pressure used in stiffened panel testing. A typical isochromatic fringe pattern at the tip of a sharp notch in the stiffener is illustrated in Figure 11. Similar patterns were also observed in the panel skin. The stress intensity factor K was computed by means of Irwin's equation[17]

$$4\tau_{max}^2 = \left(\frac{K}{2\pi r}\sin\theta + \sigma_o \sin\frac{3\theta}{2}\right)^2 + \left(\sigma_o \cos\frac{3\theta}{2}\right)^2 \qquad (5)$$

where r and θ are polar coordinates at the crack tip (Figure 11). The far-field stress σ_o and the maximum shear stress τ_{max} were determined by strain gage readings and photoelastic measurements.

Figure 12 shows the photoelastically determined stress intensity factor in the stiffener. The interesting feature is that, as the notch becomes deeper, the stress intensity increases to a maximum and then drops to lower values. A comparison of Figures 8 and 12 shows that there is a correspondence between the crack growth rate and the stress intensity factor values as a function of crack length in the stiffener.

The stress intensity factors for a cracked stiffened panel determined from the photoelastic results are presented in Figure 13. Included in the graph are the analytical results calculated by Equation (1) for Panel V. It can be seen that the analytical method gives higher K values than the photoelastic method when the crack length is short. As the crack grows into the central region of the panel, the results from both methods are practically equal. This is reasonable since the stiffener effect, which is neglected in $\Delta K_{bending}$ in Equation (1), should diminish as the crack grows away from the stiffeners. For crack length between 1.2 and 2.5 in. (30 to 64 mm), the photoelastic method gives, within the scatter of data, an approximately constant value of K = 18 ksi$\sqrt{in}$. (20 MPa$\sqrt{m}$), which is in agreement with the constant crack growth rate observed previously in Figure 9. On the other hand, the analytical method produces a gradual increase in K values from 15 to 20 ksi$\sqrt{in}$. (17 to 22 MPa$\sqrt{m}$) in the same range of crack length. Since the difference in the above K values obtained from the two methods is small, it is considered that, in spite of the simplifications, the analytical method provides adequate results for a correlation of the fatigue crack growth data.

CORRELATION OF DATA

Because failure of the stiffened panels is dependent primarily on the two central cracks growing toward each other, the ΔK_{total} and the da/dN values are computed only for these cracks in the present work. Results for the weldbonded panels are plotted in Figure 14. It is interesting to note that the data points representing the two cracks in Panel III cover a relatively wider scatter band. These were the cracks which branched during fatigue testing under a pressure of 0-8 psig (0-0.055 MPa). In general, the da/dN versus ΔK results have an acceptable scatter of data and a high degree of agreement for the three weldbonded panels tested.

The base line materials data on 5456-H343 aluminum alloy, which were obtained in a previous investigation,[18] are plotted together with the data on all five stiffened panels in Figure 15. It is evident that, on

the basis of total stress intensity by Equation (1), a correlation of the two sets of data has been achieved as they join each other and form a continuous curve. Thus, the present analytical method has been shown to be adequate for predicting fatigue crack propagation in stiffened panels from materials data which were obtained by testing simple specimens, i.e., compact tension specimens.[18] The materials data occupy the lower portion of the curve in Figure 15 because crack length measurements were not taken up to the point of rupture of the compact tension specimens; the panel data are situated at the upper portion since the cracks grew in the skin material at relatively high rates prior to fast crack propagation. The stiffened panels did not separate into two parts, and the crack lengths could be measured until the end of the tests.

REPRESENTATION OF DATA

The fracture mechanics method of characterizing fatigue crack growth behavior is to establish a relationship between da/dN and ΔK. Two equations have been developed by Chu[19]

$$\frac{da}{dN} = \frac{C(\Delta K - \Delta K_{th})^n}{[(1-R)K_c - \Delta K]^m} \tag{6}$$

and

$$\frac{da}{dN} = \frac{C(\Delta K^n - \Delta K_{th}^n)}{[(1-R)K_c - \Delta K]^m} \tag{7}$$

where ΔK_{th} is the fatigue threshold under which cracks will cease to grow, and K_c is the critical value of K for unstable crack propagation. The coefficients c, n, and m are empirically determined constants.

Since the materials data in Figure 15 indicate that the 5456-H343 alloy was insensitive to the effect of mean stresses,[18] the above two equations may be evaluated for R = 0. This is also consistent with the

loading condition of the stiffened panels. The constant ΔK_{th} may be estimated as 3.6 ksi$\sqrt{in.}$ (4 MPa$\sqrt{m}$) from Figure 15. The value of K_c is estimated as 106.8 ksi$\sqrt{in.}$ (117.3 MPa$\sqrt{m}$) from test results of a 15-in. (381-mm)-wide center-cracked specimen (Appendix). Figures 15 and 16 illustrate that the test data can be adequately represented by either of the above two equations. The empirical constants are presented in Table 3.

TABLE 3 - CRACK GROWTH EQUATION CONSTANTS

Equation	C		m	n
	English	SI		
(6)	8948	245	2.0	1.24
(7)	4045	108	2.0	1.50

CONCLUSIONS

The results of the stiffened panels tested under cyclic lateral pressure loading warrant the following conclusions:

1. In testing of weldbonded panels the stiffeners broke first. After the stiffeners broke completely, new cracks initiated and propagated in the skin. When tested without prenotches in the stiffeners, a weldbonded panel could endure more fatigue cycles than a GMA welded panel under the same pressure loading.

2. There was a stage of crack growth at approximately constant rates in the skin followed by fast crack propagation and final failure. The crack growth rate in the stiffeners increased to a peak value at about halfway through the stiffeners, and then decreased as the crack progressed toward the skin.

3. Fatigue crack growth data on stiffened panels could be correlated with base line materials data based on the approximation method of stress intensity analysis of the panels by considering the contributions due to tension and bending stresses. This method was verified by photoelastic measurements.

4. The crack growth data could be represented by the two simple equations relating da/dN and ΔK. These equations should be useful for the prediction of fatigue life of stiffened panels.

ACKNOWLEDGMENTS

The support of this work by the Naval Sea Systems Command is gratefully acknowledged. Thanks are due to Dr. H. H. Vanderveldt and Mr. C. H. Pohler for their initiation and guidance of the project, to Mr. C. C. Poe for providing his computer program, to Dr. W. E. Lukens and Mr. J. G. Macco for technical consultation and assistance, and to Mr. N. V. Marchica for his contribution to this work.

Figure 1 - Weldbonded Stiffened Panel, Spot Weld Location in Weldbonded Stiffened Panel, and Loading Conditions

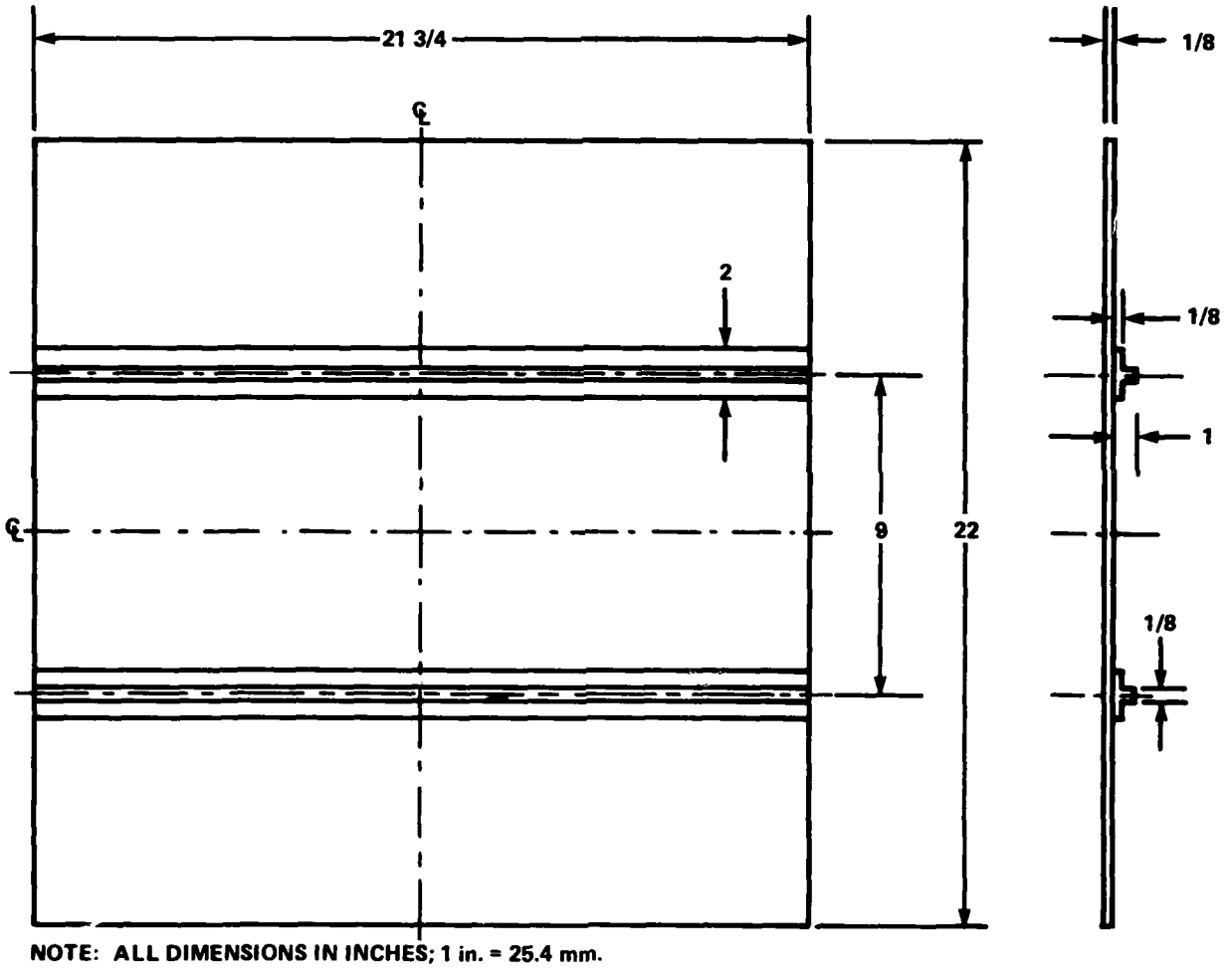

Figure 1a - Weldbonded Stiffened Panel

Figure 1 (Continued)

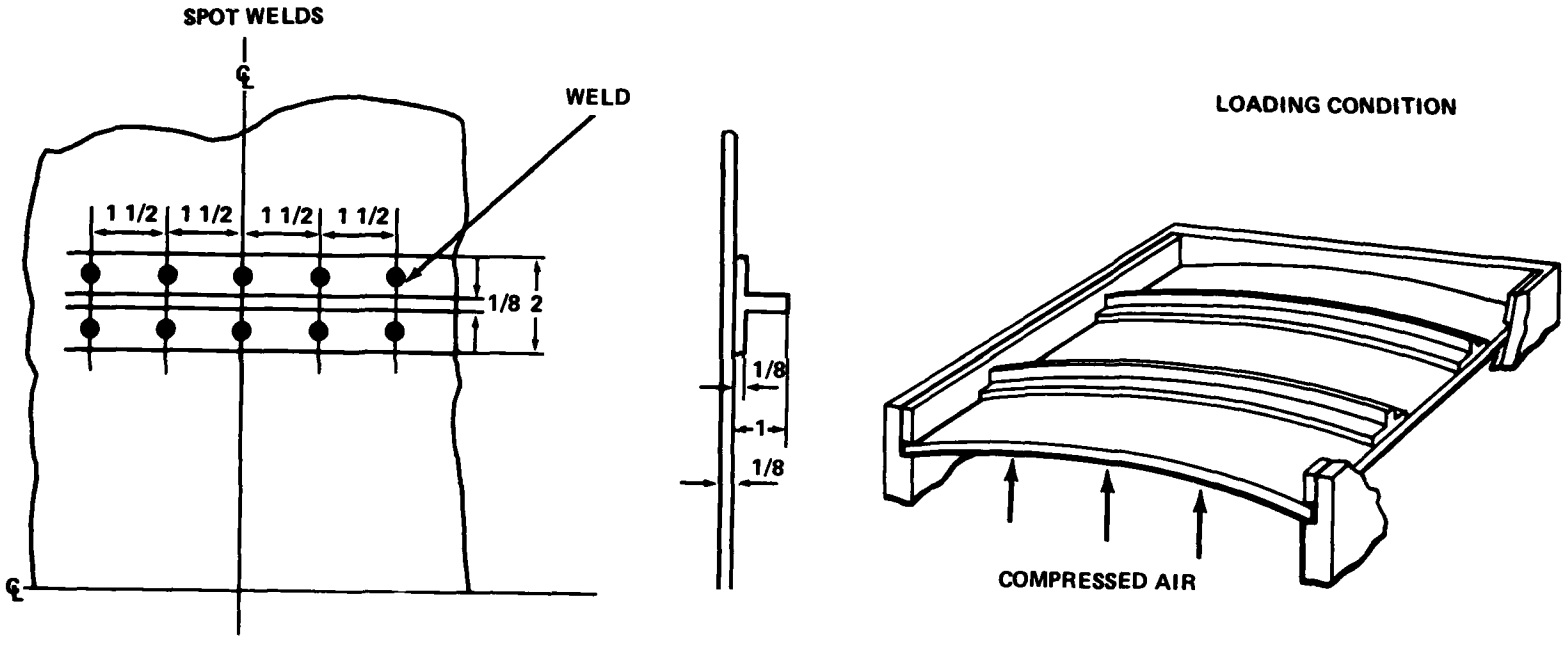

NOTE: ALL DIMENSIONS IN INCHES; 1 in. = 25.4 mm.

Figure 1b - Spot Weld Location in Weldbonded Stiffened Panel and Loading Conditions

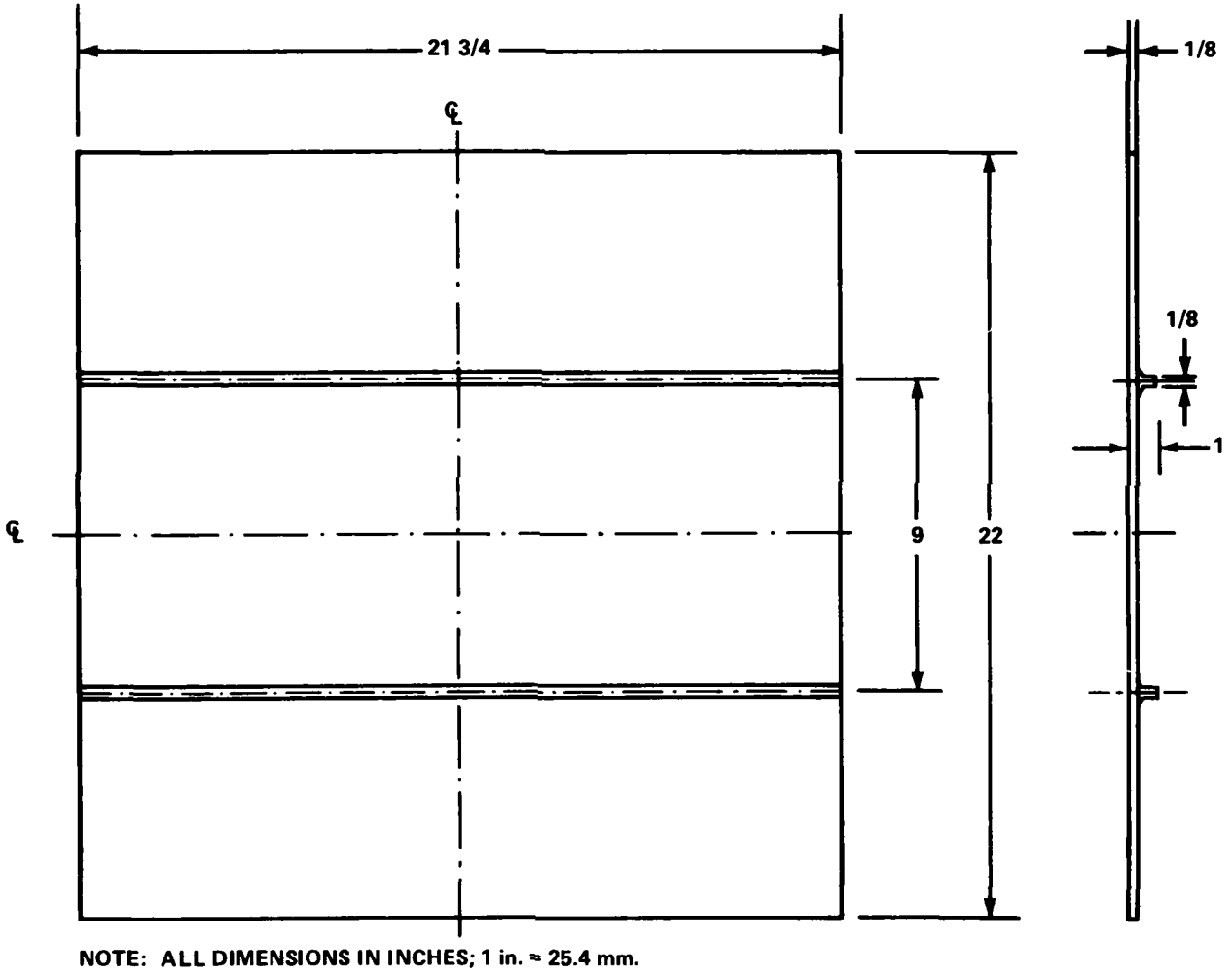

Figure 2 - Gas Metal Arc Welded Stiffened Panel

Figure 3 - Panel I After Fatigue Testing

Figure 3a - Top (Tension) Side

Figure 3 (Continued)

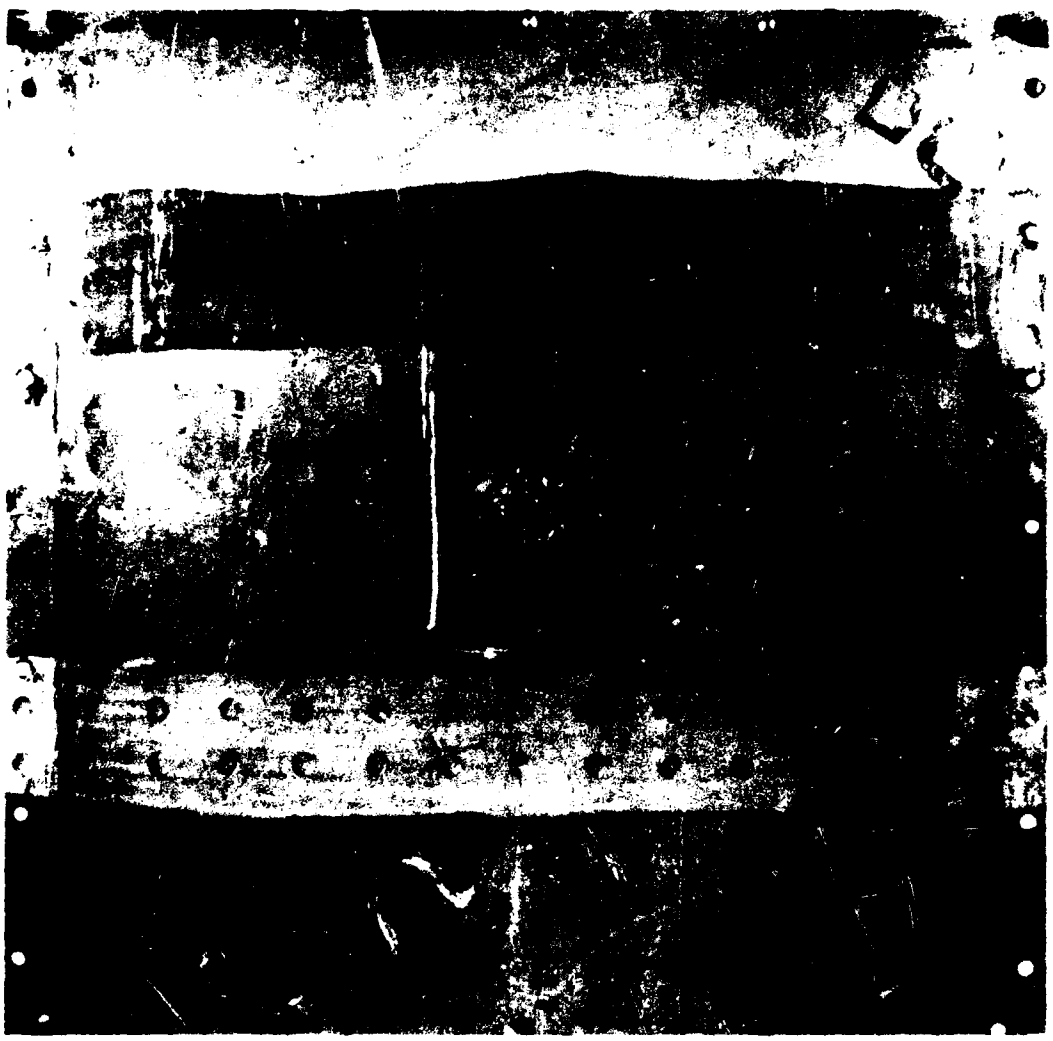

Figure 3b - Bottom (Compression) Side

Figure 4 - Panel II After Fatigue Testing

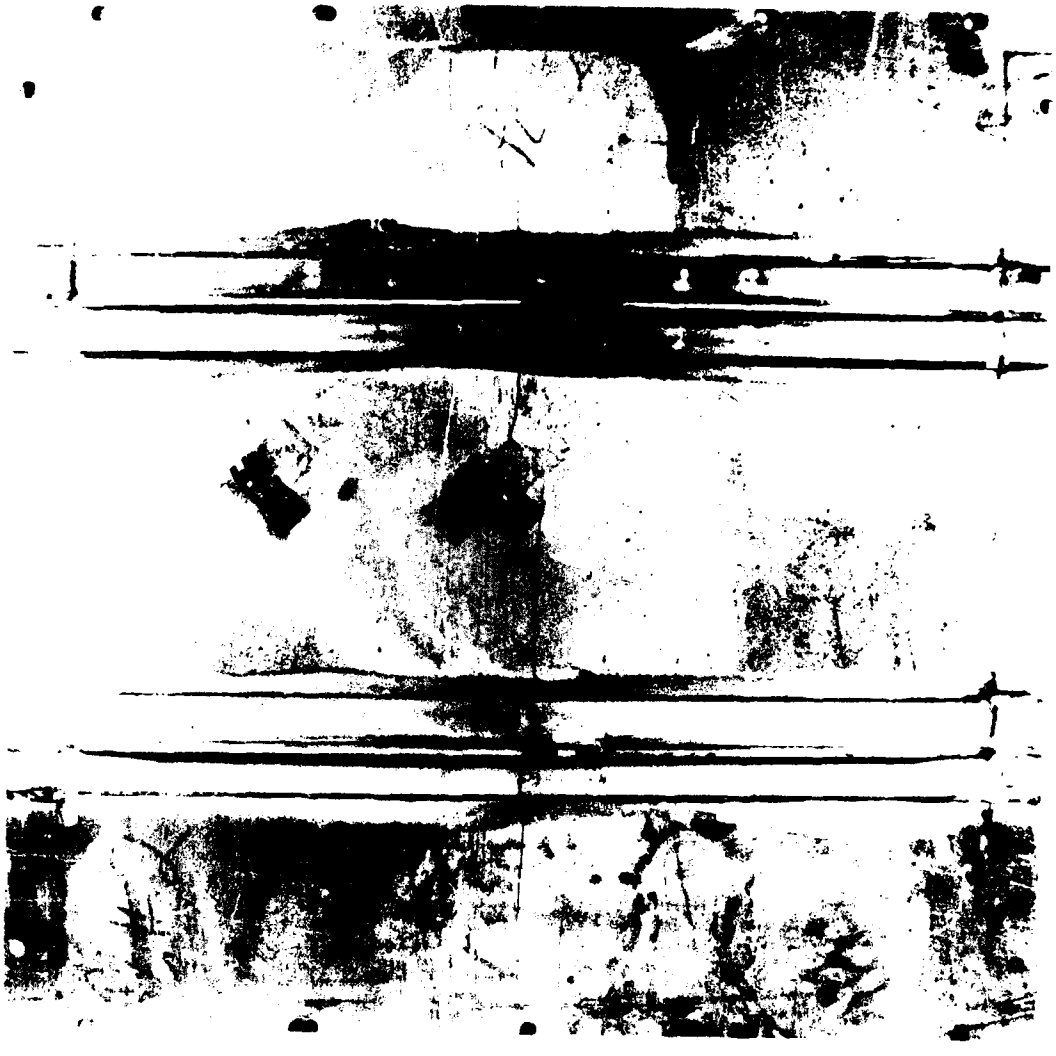

Figure 4a - Top (Tension) Side

Figure 4 (Continued)

Figure 4b - Bottom (Compression) Side

Figure 5 - Panel III After Fatigue Testing

Figure 5a - Top (Tension) Side

Figure 5b - Bottom (Compression) Side

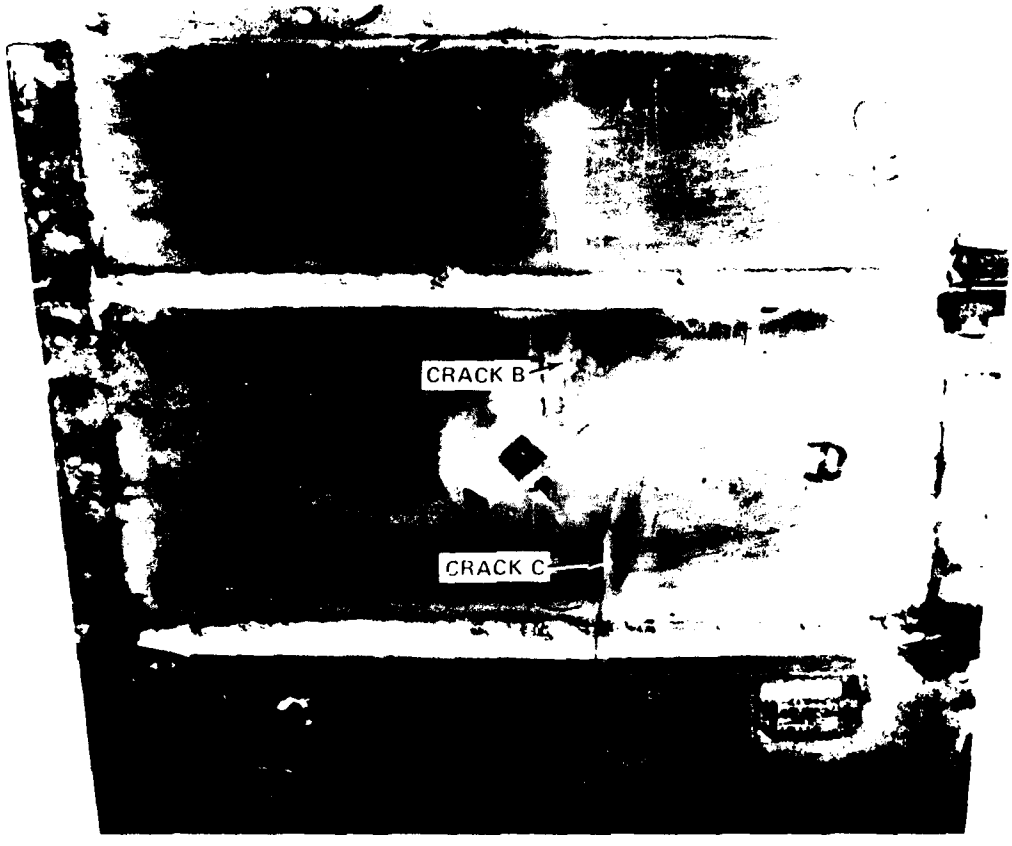

Figure 6 - Panel IV After Fatigue Testing

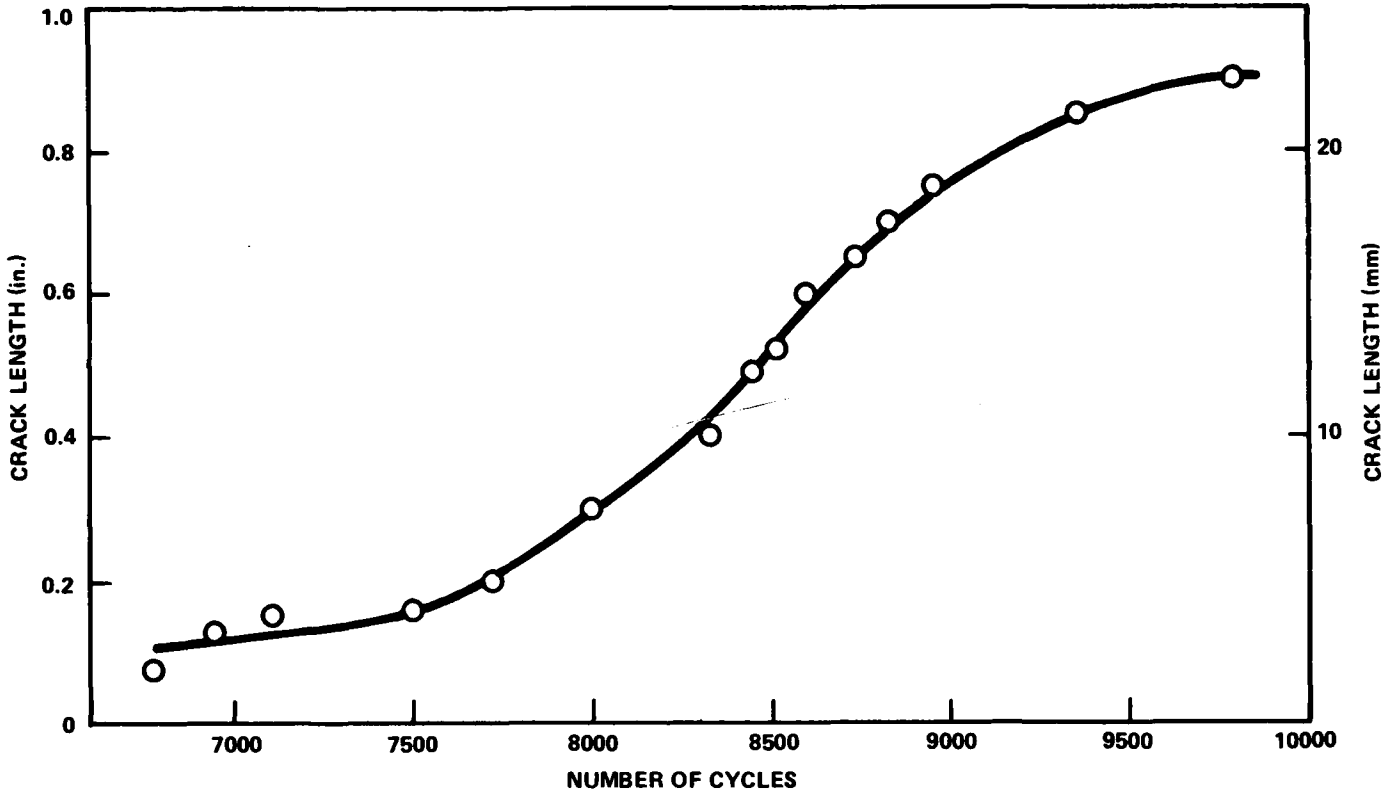

Figure 7 - Fatigue Crack Growth Measurements in a Prenotched Stiffener of Panel III

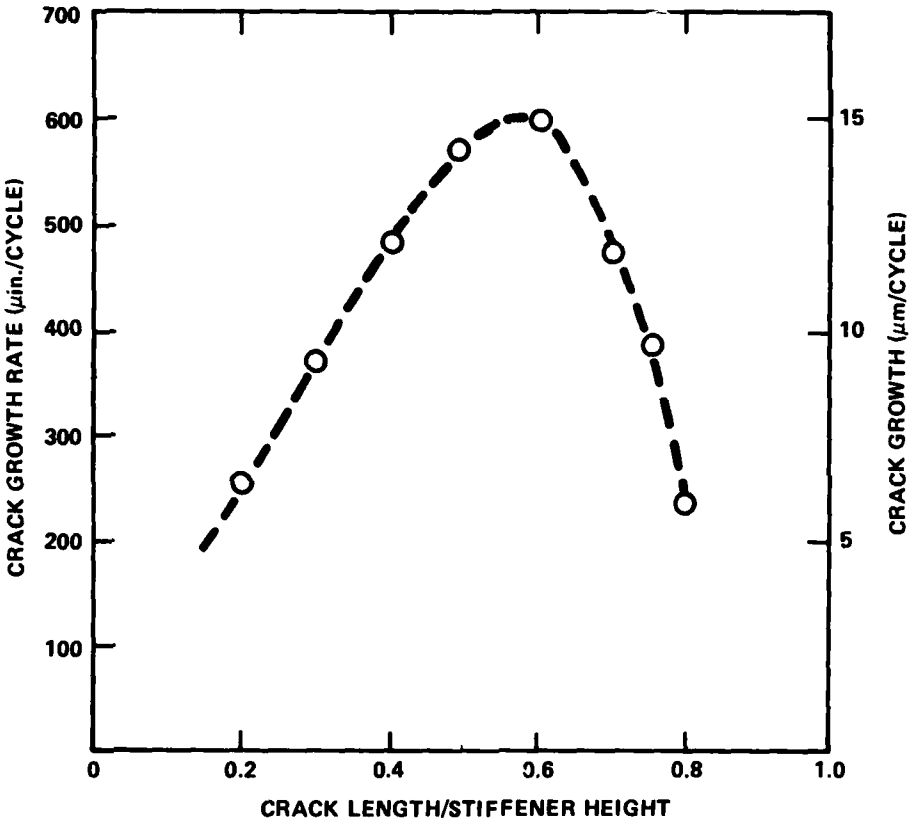

Figure 8 - Crack Growth Rate da/dN, Computed from Data in Figure 7, in a Prenotched Stiffener of Panel III

Figure 9 - Crack Growth Measurements in the Skin of Panels I and IV Under Pressure Loading of 0-20 psig (0-0138 MPa)

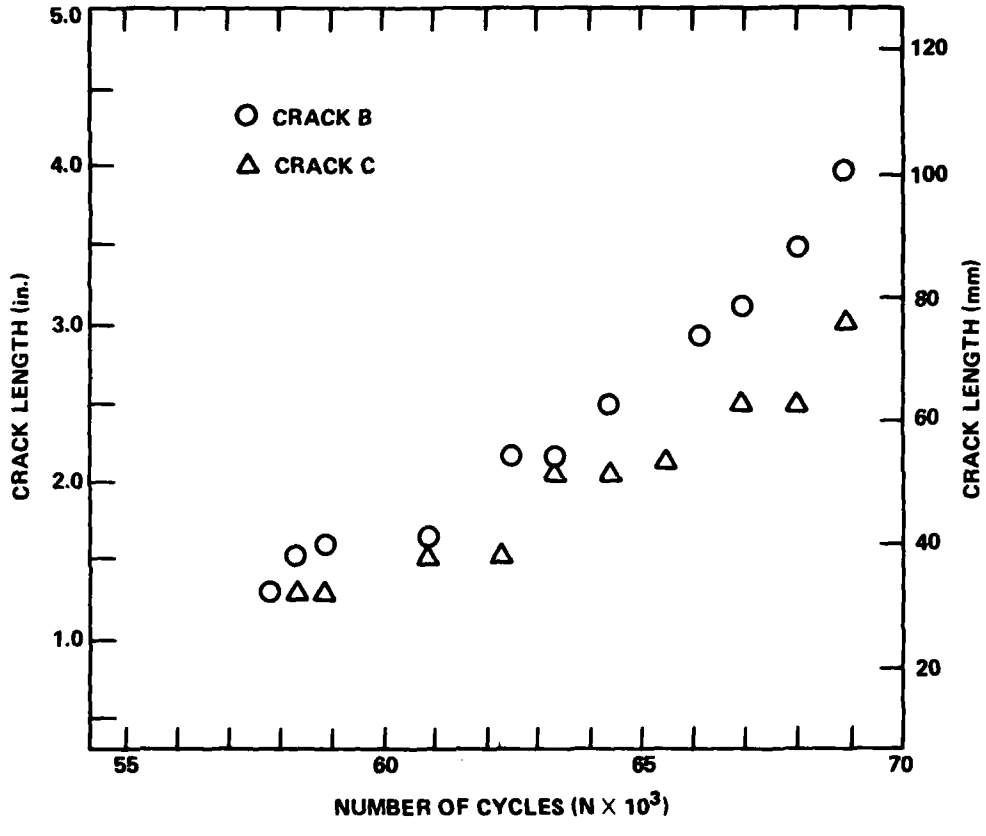

Figure 9a - Panel I (Weldbonded)

Figure 9 (Continued)

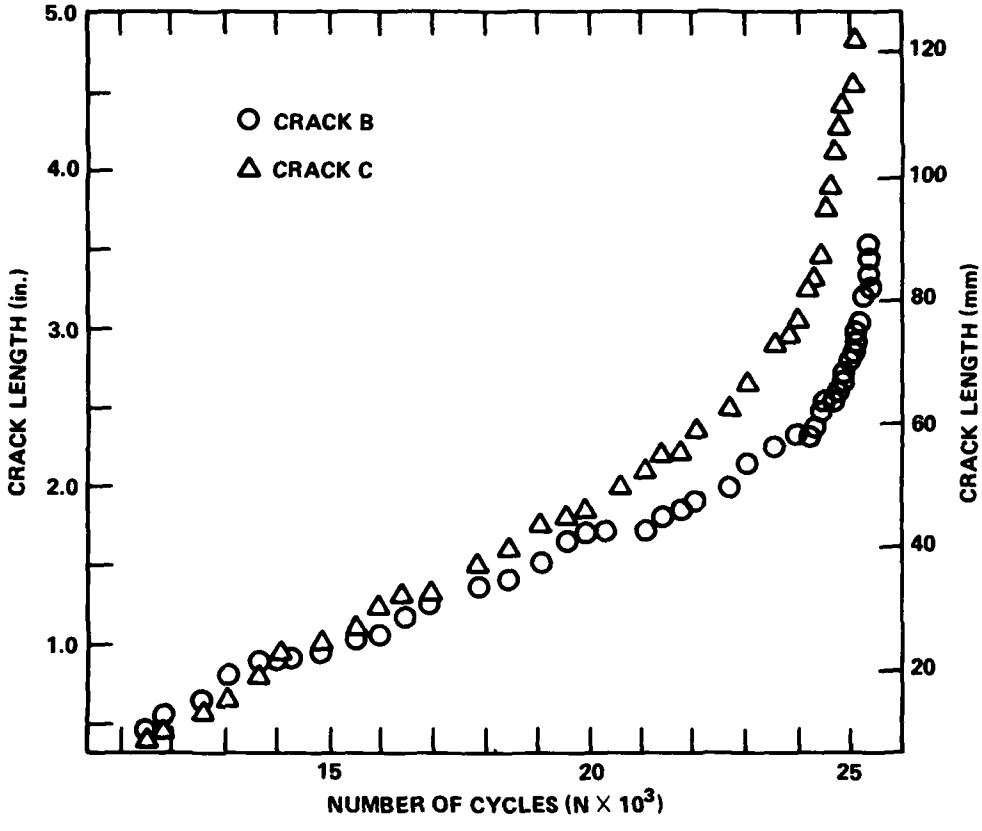

Figure 9b - Panel IV (Gas Metal Arc Welded)

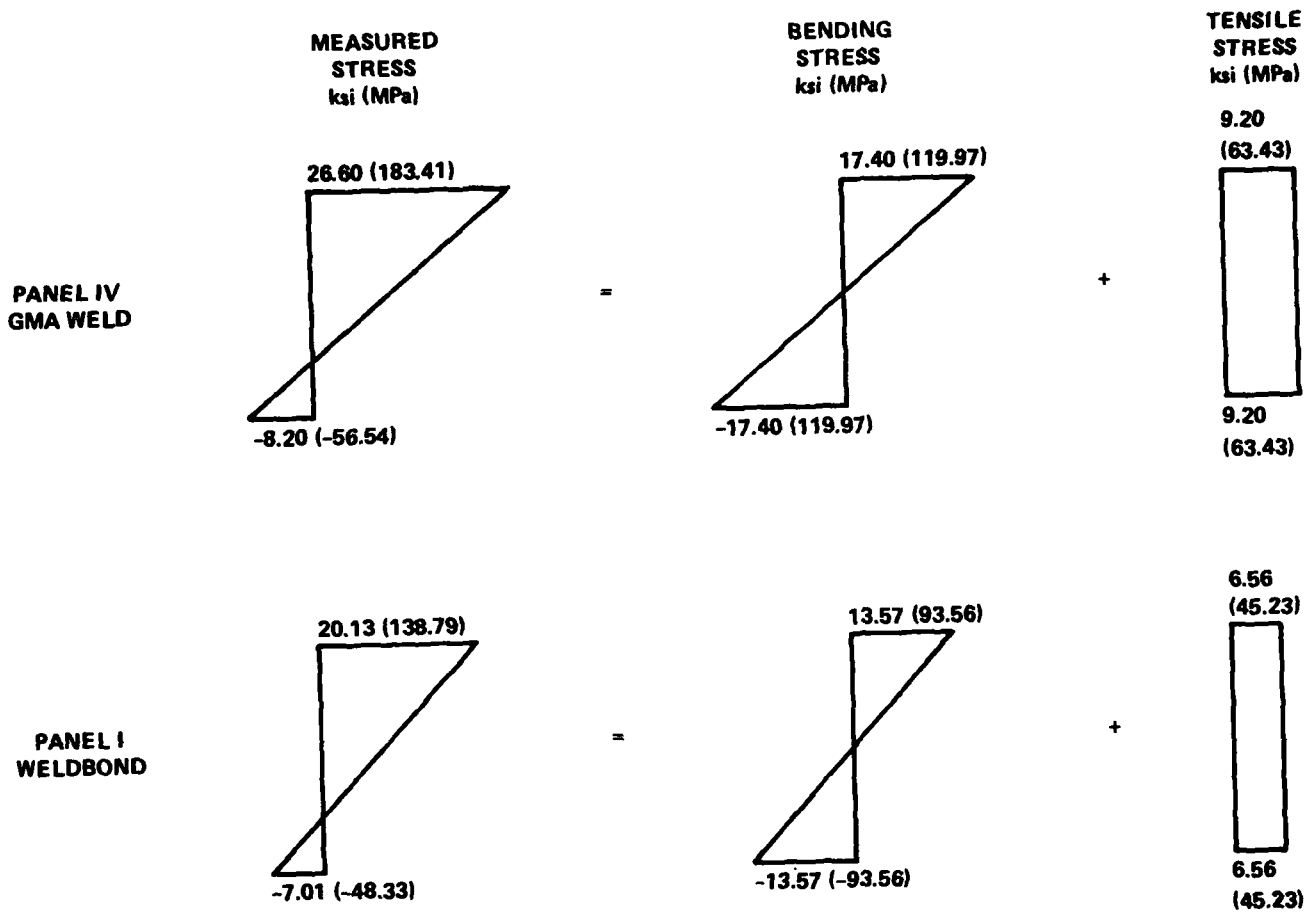

Figure 10 - Examples of Tensile and Bending Stress Computations from Measured Stresses

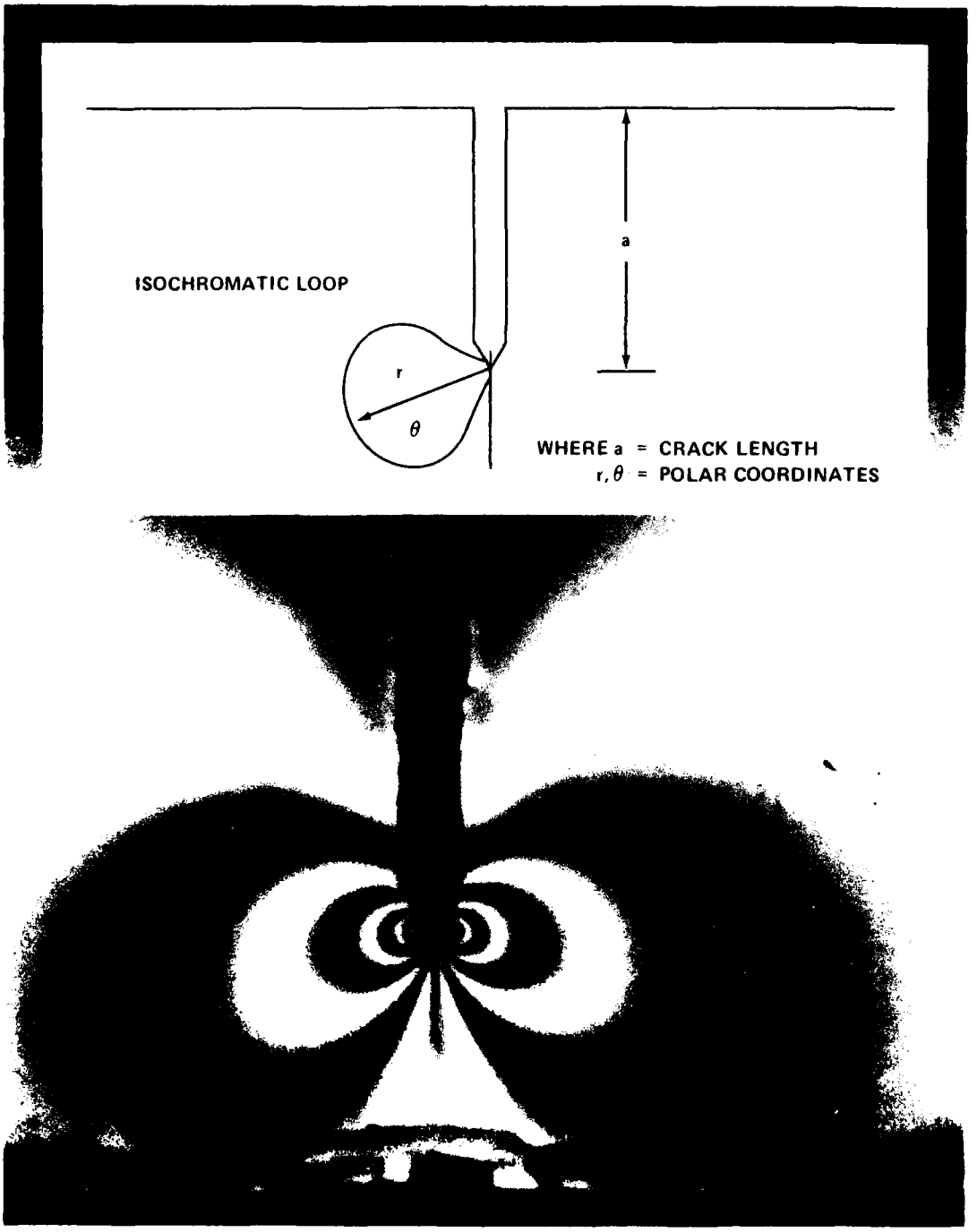

Figure 11 - Typical Isochromatic Fringe Pattern
of Crack in Stiffener

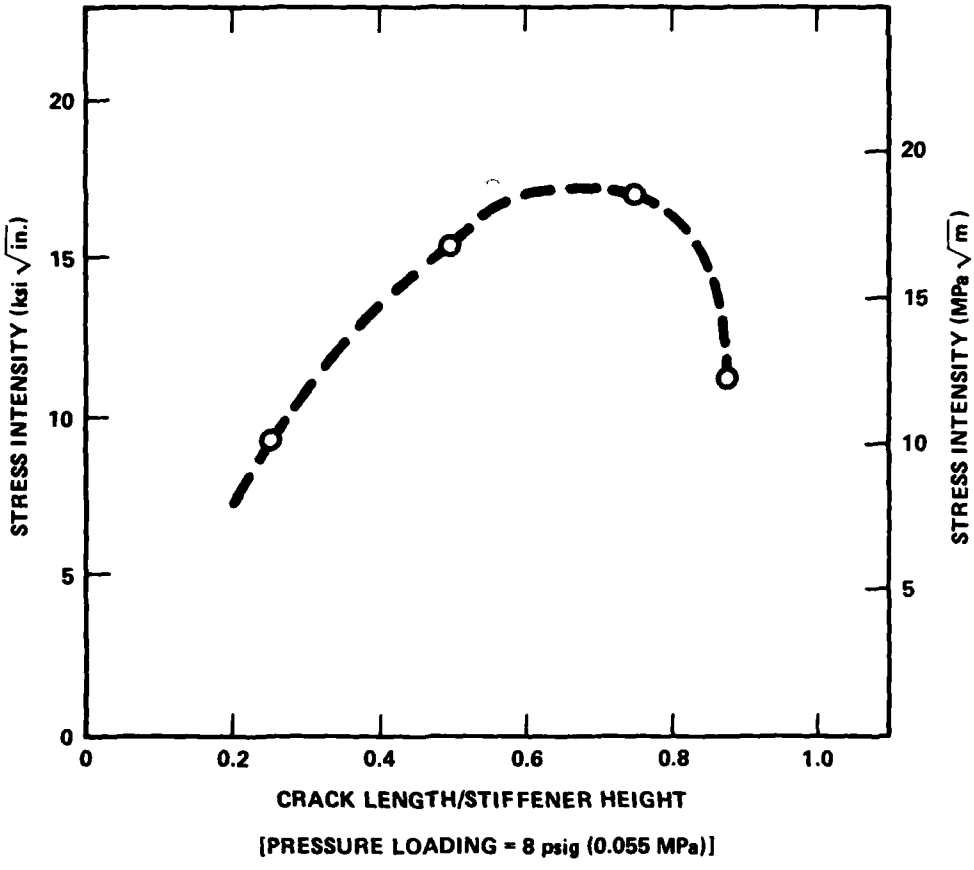

Figure 12 - Stress Intensity Factor K of a Cracked Stiffener from Photoelastic Measurements

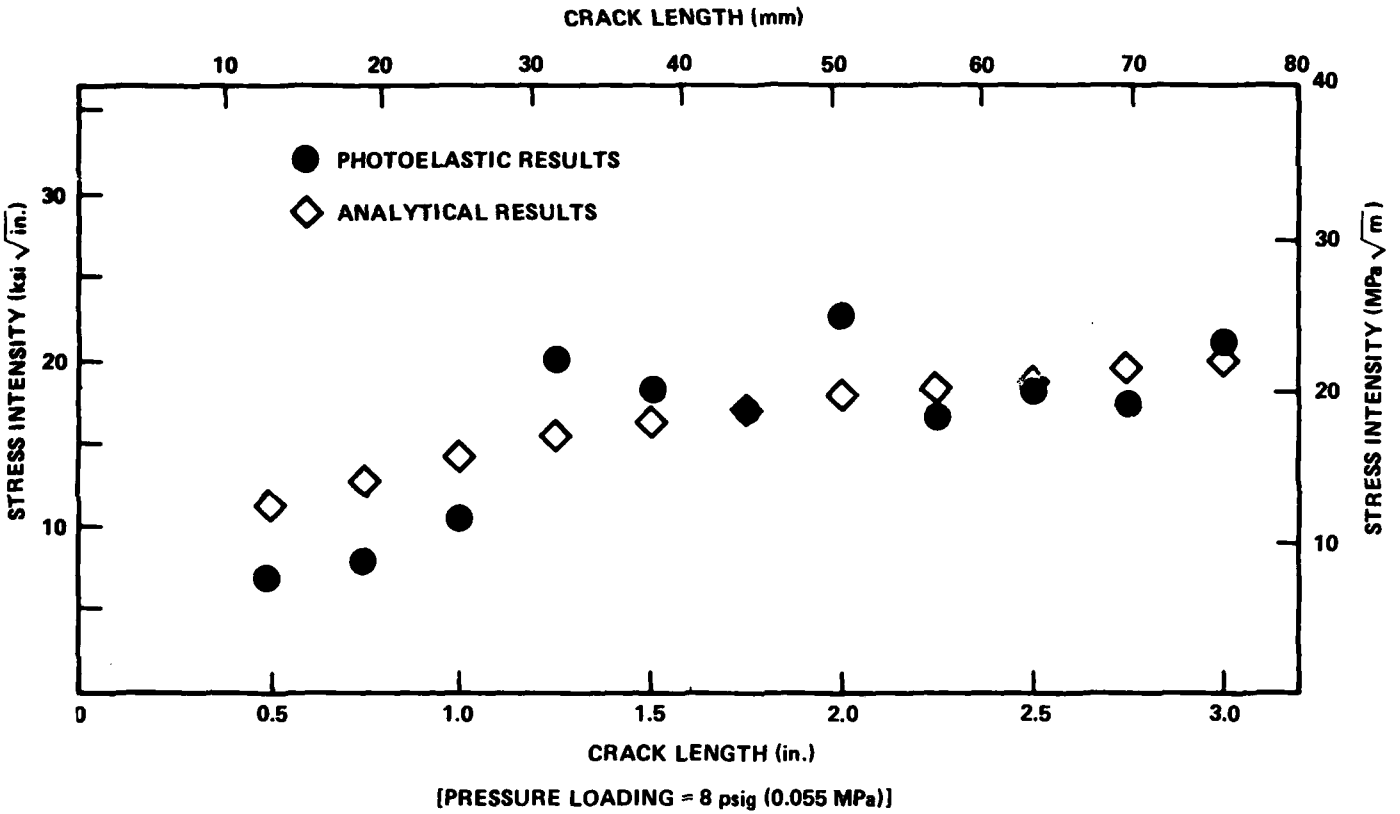

Figure 13 - Stress Intensity Factor K Along Center Line in the Central Region of a Cracked Stiffened Panel

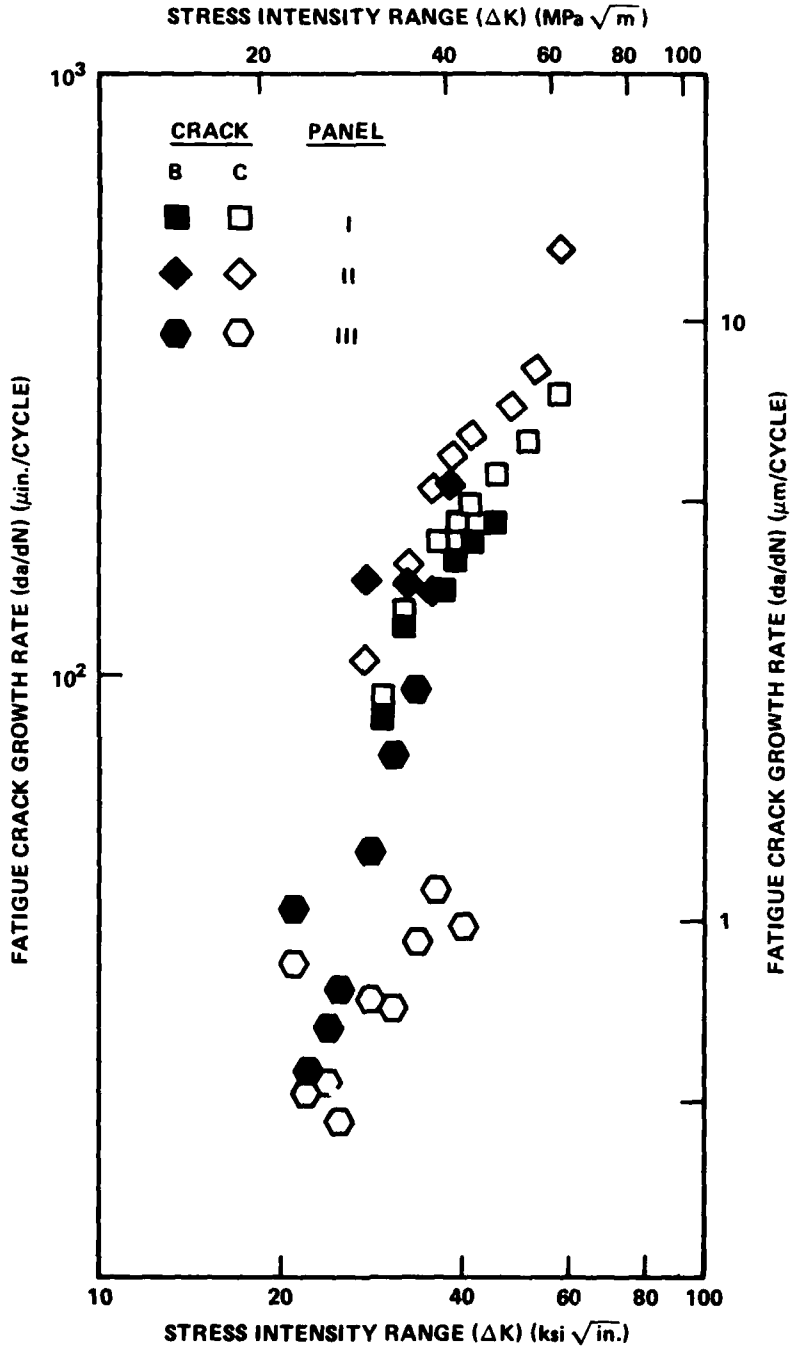

Figure 14 - Fatigue Crack Growth Rate Versus Stress Intensity Range of Weldbonded Stiffened Panels

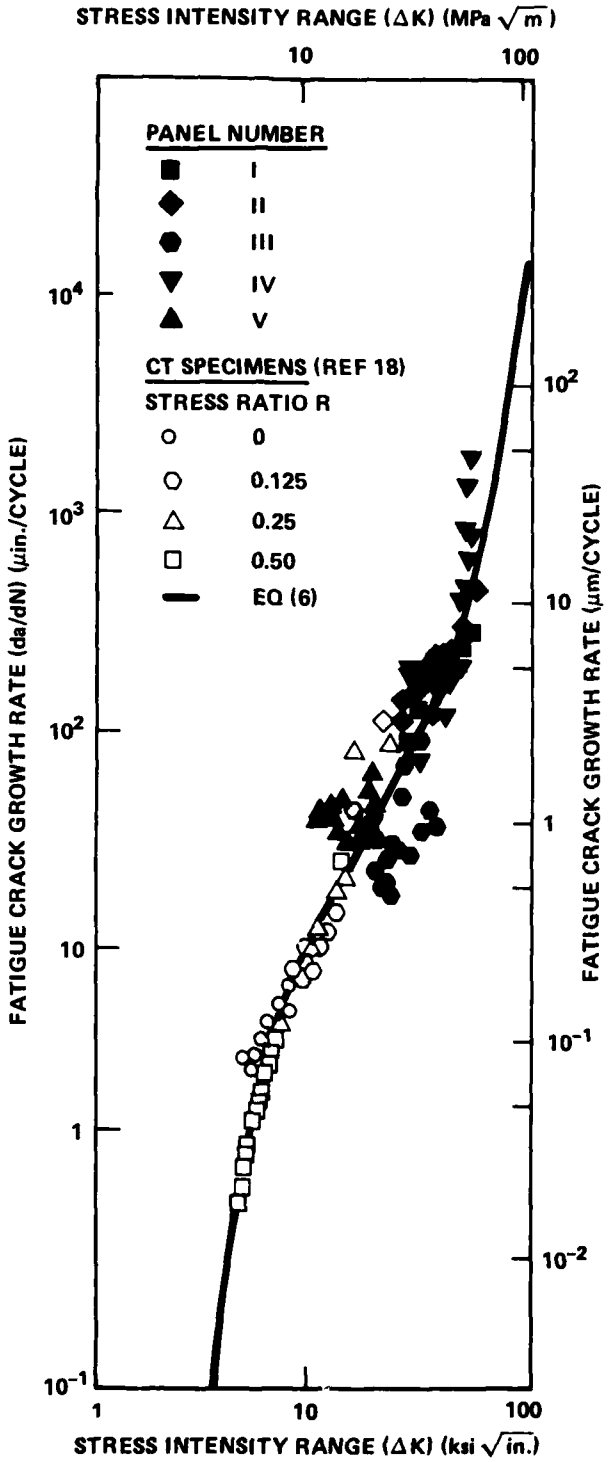

Figure 15 - Correlation of Fatigue Crack Growth Rate Results of Stiffened Panels and Base Line Materials Data of Compact Tension Specimens

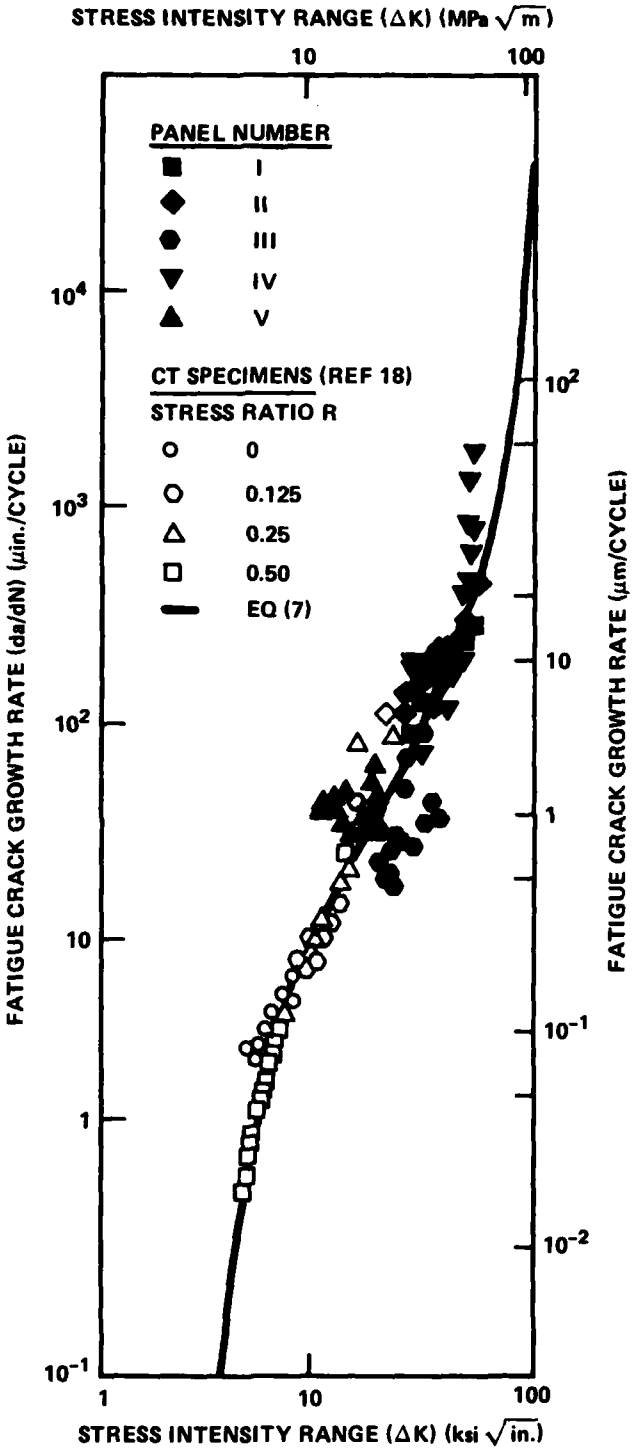

Figure 16 - Correlation of Fatigue Crack Growth Rate Results of Stiffened Panels and Base Line Materials Data of Compact Tension Specimens

APPENDIX

THE ESTIMATION OF K_c OF THE 5456-H343 SHEET ALUMINUM ALLOY

The fracture toughness K_c value of the 5456-H343 aluminum alloy was needed for Equations (6) and (7), so that crack growth in the stiffened panels could be predicted up to unstable crack propagation. The K_c value was measured by testing a 15-in. (381-mm)-wide specimen with a center notch of 4.50 in. (114.3 mm), which was oriented in the rolling direction of the sheet alloy. After fatigue precracking, the specimen was tested in an MTS machine at a strain rate of 0.2 percent per minute. A load versus crack opening displacement curve was recorded, and the effective crack length was determined from this curve according to ASTM recommended procedure.[20]

The crack extension behavior of the specimen under tensile loading followed a typical pattern observed by Sullivan et al.[21] As shown in Figure 17, the crack, at first, maintained its initial length under rising load (Region I). Slow stable crack growth occurred as the load was further raised (Region II). In this region, if the load was held constant, the crack would cease to grow. Finally, the load reached the maximum and stayed at a constant level while the crack grew at an accelerating rate until rupture (Region III). Sullivan suggested that the starting point of Region III is the limit of structural integrity, and the effective crack length at this location and the maximum load should be used to calculate fracture toughness K_c of the material. The fracture toughness was computed by this method as K_c = 106.8 ksi$\sqrt{\text{in.}}$ (117.3 MPa$\sqrt{\text{m}}$) by the use of Feddersen's formula[22] for center-notched specimens.

It should be noted that this was an estimation of the K_c value and that the 5456-H343 aluminum alloy was apparently a tough material. A simple calculation revealed that the net section stress of the specimen at failure was 53.3 ksi (367.7 MPa), which was about equal to the tensile strength of the alloy. It indicates that the 15-in. (381-mm)-wide specimen sustained a considerable amount of plastic deformation before rupture.

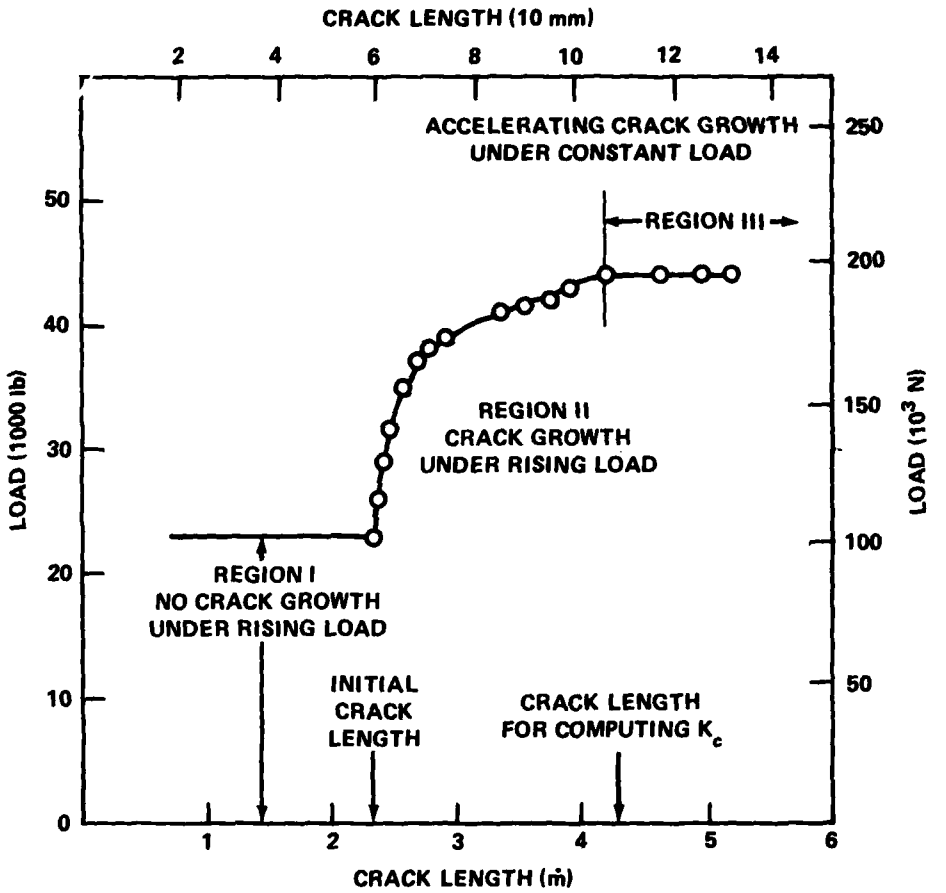

Figure 17 - Crack Extension in the Center-Notched Tension Specimen

REFERENCES

1. Poe, C. C., "Fatigue Crack Propagation in Stiffened Panels," ASTM STP 486, pp. 79-97 (1971).

2. Vlieger, H., "The Residual Strength Characteristics of Stiffened Panels Containing Fatigue Cracks," Engineering Fracture Mechanics, Vol. 5, No. 2, pp. 447-477 (Jun 1973).

3. Sorkin, G., et al., "An Overview of Fatigue and Fracture for Design and Certification of Advanced High Performance Ships," Engineering Fracture Mechanics, Vol. 5, No. 2, pp. 307-352 (Jun 1973).

4. Wolfe, R. J., et al., "Some Considerations of Fracture-Mechanics Applications in Ship Design, Construction and Operation," Engineering Fracture Mechanics, Vol. 7, No. 3, pp. 565-581 (Sep 1975).

5. Paris, P. C., "The Fracture Mechanics Approach to Fatigue," Proceedings, 10th Sagamore Army Materials Research Conference, Syracuse University Press, pp. 107-132 (1964).

6. Wei, R. P., "Fracture Mechanics Approach to Fatigue Analysis in Design," Journal of Engineering Materials and Technology, Vol. 100, pp. 113-120 (Apr 1978).

7. Lukens, W. E., "Fatigue Behavior of Aluminum Alloy Weldments and Panels," Presented at the Golden Gate Welding and Metals Conference, San Francisco, California (Jan 1975).

8. Cordiano, H. V., "Effect of Residue Stresses on the Low Cycle Fatigue Life of Large Scale Weldments in High Strength Steel," Journal of Engineering for Industry, Vol. 92, No. 1, pp. 86-92 (Feb 1970).

9. Chu, H. P., et al., "Fatigue Crack Propagation in Aluminum Alloy Stiffened Panels Under Uniform Lateral Loading," SESA Paper D-23, Presented at SESA Spring Meeting, Dallas, Texas (May 1977).

10. Irwin, G. R., "Comments on Dynamic Fracturing," ASTM STP 627, pp. 7-18 (1977).

11. "A Digest of Tentative Standard Method of Test for Fatigue Crack Growth Rate in Metallic Materials," ASTM Task Group E24.04.01 (Jul 1975).

12. Craddock, J. M., "Weldbonding/Rivetbonding: Application Testing of Thin Gauge Ai-craft Components," AIAA Paper No. 73-805 (1973).

13. Haughey, V. A., "Improved Approach to Structural Integrity of Spacecraft Shrouds by Use of Skin-Corrugated Weldbond," AIAA Paper No. 74-381 (1974).

14. Sih, G. C., "Handbook of Stress Intensity Factors," Lehigh University Press (1973).

15. Tada, H., et al., "The Stress Analysis of Cracks Handbook," Del Research Corp. (1973).

16. Poe, C. C., "The Effect of Broken Stringers on the Stress Intensity Factor for a Uniformly Stiffened Sheet Containing a Crack," Presented at the 10th Anniversary Meeting of the Society of Engineering Science, Raleigh, North Carolina (Nov 1973).

17. Irwin, G. R., "The Dynamic Stress Distribution Surrounding a Running Crack - A Photoelastic Analysis," SESA Proceedings, Vol. 16, No. 1 (1958).

18. Chu, H. P., et al., "Fatigue Crack Growth in 5456-H343 Aluminum Alloy," Presented at the AIME Annual Meeting, Denver, Colorado (26 Feb - 2 Mar 1978).

19. Chu, H. P., "Effect of Mean Stress Intensity on Fatigue Crack Growth in a 5456-H117 Aluminum Alloy," ASTM STP 559, pp. 245-260 (1974).

20. "ASTM Proposed Recommended Practice for R-Curve Determination," Annual Book of ASTM Standard, Part 10, pp. 669-683 (1974).

21. Sullivan, A. M., et al., "Comparison of R-Curves Determined from Different Specimen Types," ASTM STP 527, pp. 85-101 (1973).

22. Feddersen, C. E., "Plane Strain Crack Toughness Testing of High Strength Metallic Materials," ASTM STP 410, pp. 77-79 (1967).

INITIAL DISTRIBUTION

Copies	
2	ONR
	1 Code 439
	1 Code 471
3	NRL
	1 Code 6382
	1 Code 6384
	1 Code 8430
7	NAVSEA
	1 SEA 05D
	2 SEA 05R/Vanderveldt
	2 SEA 32R/Pohler
	2 SEA 99612
12	DTIC

CENTER DISTRIBUTION

Copies	Code	Name
1	17	W. Murray
1	172	M. Krenzke
1	173	A. Stavovy
1	1730.2	N. Nappi
1	1730.5	J. Adamchak
5	1730.5	J. Sikora
5	1730.6	J. Hauser
1	1730.6	A. Stavovy
1	2802	I. Kramer
1	2803	J. Kelly
5	281	G. Wacker
10	2814	H. Chu
1	2814	J. Gudas
1	282	J. Crisci
1	2822	W. Lukens
10	5211.1	Reports Distribution
1	522.1	Unclass Lubrary (C)
1	522.2	Unclass Library (A)
2	5231	Office Services